THE LNLS 500 MeV BOOSTER SYNCHROTRON

R.H.A. Farias, M.J. Ferreira, Liu Lin, A.C. Lira, C. Pardine, P.F. Tavares* and G. Tosin,
LNLS, Campinas, Brazil

Abstract

We present the current status of the construction and tests of components of a 500 MeV booster synchrotron to be used as an injector for the 1.37 GeV electron storage ring at the Brazilian Synchrotron Light Source (LNLS). Increased user demand for higher currents and also for the installation of insertion devices has led us to shorten the booster construction schedule and we now plan to have all subsystems installed by the end of 2000. Machine commissioning will start in January 2001.

1 INTRODUCTION

The Brazilian National Synchrotron Light Laboratory (LNLS) operates a 1.37 GeV electron storage ring with a 120 MeV injector LINAC. The light source has been operating routinely for users since July 1997 and during that time all design specifications have been met or surpassed: a maximum of 188 mA of stored current (@ 1.37 GeV), 14 hours of lifetime (@ 100 mA), and orbit stability (in the vertical plane) better than ±5 µm along users shifts. The decision to upgrade the injection energy arose from the need to install small gap insertion devices and also to further increase the stored beam current by improving the injection efficiency. Table I shows the main machine parameters. A detailed account of the machine conceptual design and the rationale for the choice of the main parameters was given in previous work [1]. In this report, we concentrate on experimental results on the booster magnet characterization (as well as its impact on accelerator physics considerations), pulsed magnets, RF system and power supplies.

2 BOOSTER DIPOLE MAGNET OPTICAL MODEL

The model for the dipole magnetic field has to be carefully considered for small rings. Effects from the finite extent of fringe fields or small curvature radius may not be negligible as compared to the effects of the hard-edge model. Not only the lattice design had to be re-evaluated in face of the dipole prototype measurement results but also the prototype requirements were re-defined after more accurate lattice design, in an interactive way. The rectangular hard-edge dipole model provides vertical focusing of the beam at entrance and exit edges given by

$$\frac{1}{f_y} = \frac{1}{\rho}\tan(\beta)$$

where ρ is the radius of curvature, θ is the deflection angle and $\beta=\theta/2$. For small ρ, the contribution from the dipole edge to the vertical focusing can be comparable to that of the quadrupoles in the lattice. For the LNLS booster we have ρ=1.02598 m and θ=30º, which gives us $1/f_y$=0.26 m^{-1}. This is about 40% of the value of the strongest quadrupole. In fact, in the booster lattice all quadrupole magnets in the dispersive arc (containing six dipoles) are horizontally focusing. All vertical focusing comes from the dipole edges. The finite extent of the fringe field introduces a correction term to the rectangular dipole vertical edge focusing:

$$\frac{1}{f_y} = \frac{1}{\rho}\tan(\beta-\psi), \quad \psi = K\frac{g}{\rho}\sec\beta\left(1+\sin^2\beta\right)$$

where g is the magnet gap and the form factor K is

$$K = \int_{-\infty}^{+\infty}\frac{B_y(z)\left[B_0 - B_y(z)\right]}{g\,B_0^2}\,.$$

Table I: Injector ring main parameters.

Maximum energy	500	MeV
Injection energy	120	MeV
Circumference	34.0	m
RF frequency	476.0	MHz
Horizontal tune	2.27	
Vertical tune	1.16	
Horizontal natural chromaticity	-2.1	
Vertical natural chromaticity	-2.5	
Repetition rate	0.2	Hz
Current (@ 500 MeV)	70	mA
Storage ring filling time (300 mA)	2	min
Dipoles	12	
Quadrupoles	18	
Sextupoles	8	
Steering magnets (H/V)	10/6	
BPMs	12	

$B_y(z)$ is the magnitude of the fringe field on the magnetic midplane at position z and B_0 is the value of $B_y(z)$ at the center of the magnet. Numerical integration performed along the electron's trajectory for the measured prototype field gives values for K ranging from 0.64 to 0.71, depending on the excitation current and shim profile. This corresponds to losing about 20% of the vertical focusing strength as compared to the hard-edge model. The main consequence for the linear optics is the increase of the maximum dispersion function in the arcs, which, in turn, decreases the energy acceptance of the booster for a given

* e-mail: pedro@lnls.br

vacuum chamber aperture. We decided then to shape the shim profile at the dipole extremities to introduce additional vertical focusing. In order to produce a model for the dipole that could represent correctly its field distribution, with finite extent for the fringe field and quadrupolar gradient profile produced by dipole face inclination and shims, a code for numerical tracking of electrons through the measured magnetic field has been developed using Mathematica.™ The first order transfer matrix is calculated numerically and the results are compared to the transfer matrix given by a model composed by 1000 small sector dipoles with field index. The results agree well and this model is adopted for linear beam dynamics calculations, since it is conveniently adapted to existing beam dynamics codes (e.g. MAD). We have used the magnetic measurement results for the dipole without shims as a first estimate for the effects of the 'real' dipole on the beam optics. A scaling factor for the quadrupolar gradient profile was used as a variable parameter for optics matching. The integrated gradient obtained after lattice optimization has been used as a first goal for the dipole shim profile. The final shim produces an integrated quadrupolar gradient which is larger than the one given by the hard-edge model by 20%.

3 BOOSTER MAGNETS CONSTRUCTION

All booster magnets (as all other DC magnets in the storage ring) are made from laser-cut 1.5 mm thick low-carbon steel laminations and were designed and built at LNLS.

The booster dipoles are rectangular 30 degree bending magnets that produce up to 1.67 T. In order to reduce the magnet weight (limited by the available crane capacity) and provide for easy installation of light ports for beam diagnostics and future experiments, the magnet is C-type and the laminations are staggered. Two booster dipole magnet prototypes were built and detailed field maps were used to determine the pole shims necessary to achieved the desired integrated field profile. Care was also taken to guarantee that the physical and magnetic length of the booster dipoles match the design specifications so as to provide the correct booster revolution frequency (and the corresponding RF frequency, which is the same as the storage ring rf frequency). This required computer control of the lamination cutting procedure so as to ensure that, despite lamination thickness irregularities, the total dipole length is correct to within less than a mm. In fact, the laser cutting procedure is especially convenient for the fabrication of the dipole magnets, since it allows the use of tie rods for the assembly of the magnet laminations (instead of welding). In order for this to be possible, given the fact that the dipole laminations are staggered, the holes for the tie-rods must be cut in different positions in each lamination, a method only feasible with laser cutting.

The booster quadrupoles reach a maximum gradient of 6 T/m with a bore diameter of 54 mm and the power dissipation in the coils is only 88 watts, so that water cooling is not needed. In August 1999, after testing three different prototypes, series production of the 18 booster quadrupoles was started. By the end of the year all of them were ready to be characterized along with the 8 booster sextupoles.

4 MAGNET POWER SUPPLIES

The booster repetition rate is low enough (0.2 Hz) that current controlled power supplies are capable of overcoming the relatively low magnet inductance in a total ramping time of 3 seconds. The dipole power supply is the largest one and must provide 300 A of current at 31 volts per magnet. In order to reduce the time needed for the whole booster cycle, the time constant of the magnet is reduced during the current fall time by switching a resistor in series with the magnets. The design repetition rate has thus been achieved with a prototype supply (which takes a single magnet as its load).

The quadrupole and sextupole power supplies use an isolated high frequency (45 kHz) switched-mode AC/DC converter input stage that provides a stabilized output voltage that varies according to the load current. This input stage drives a switched-mode buck chopper stage. The main advantage of this design (as compared to the topology used in the storage ring power supplies, made up of a 60 Hz transformer followed by a controlled rectifier) is that the use of high frequency components makes the supply much more compact for a given output power also reducing mechanical assembly costs and time. The control stage is based upon stabilization by output current limitation, the voltage delivered by the AC/DC converter being adjusted such that the switching frequency is always maximum and the chopper transistor in the switching module works at 50% duty cycle. The AC/DC converter modules were designed and prototypes were tested at LNLS but series production was contracted out to local industry which delivered all modules by the end of 1999.

5 PULSED MAGNETS

The most challenging of the pulsed magnets for the booster is the ejection kicker. In order to achieve adequate extraction efficiency from the booster, the risetime of the current pulse in this magnet must be short compared to the booster revolution period, which is only 113 ns. The design rise time for the kicker is 30 ns and the magnet has been divided into two sections (so as to reduce the magnet inductance) and two thyratron tubes must fire in synchronism to produce the desired deflection of 6 mrad to the 500 MeV beam. Prototype work done up until now (using a single thyratron pulsing half of the final kicker) using the pulser circuit in Figure 1 has reached 36 ns risetime with an acceptable overshoot.

The booster injection kicker is of similar construction (window frame in-vacuum ferrite core magnet) but the necessary fall time and peak current are much more relaxed. A single kicker will be used to perform on axis injection into the booster.

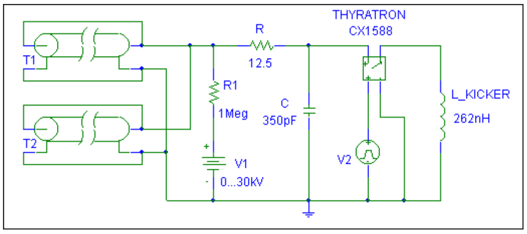

Figure 1: Prototype kicker pulser circuit.

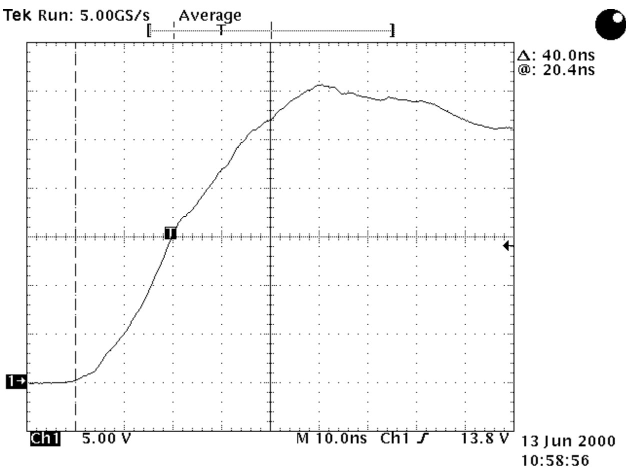

Figure 2 Current waveform in the prototype booster extraction kicker. 20% current overshoot and a 36 ns (5 to 95%) risetime are observed. (65 Amp/div)

All 5 septa (thin and thick) in the LINAC to booster and booster to storage ring transport lines share the same basic design with a C-type ferrite core design and a single turn coil and differ only in length and maximum field. Shielding of the septum field is achieved with an active septum configuration with additional shielding provided by a copper tube around the booster/storage ring vacuum chamber. The design for all septa pulsers (based on thyristor switches) is finished and a prototype has been built and tested. Preliminary measurements of the leakage fields in a prototype septum have shown the need to add passive shielding (in the form of a thicker copper tube) in order to achieved the design specifications.

6 RF SYSTEM

Given the relatively low RF power requirements of the booster (less than a kW), solid state power amplifiers are being developed as a cost effective alternative to a commercial klystron or tetrode tube. This development has benefited greatly from the expert advice of RF engineers at the Synchrotron Radiation Facility LURE, in France [2]. By the end of 1999, a prototype amplifier module reached a record of 250 W CW power. (cf. Figure 4) with 60% efficiency @ 476 MHz. 9 modules will be used to produce up to 1.6 kW and at this time a power combiner is being built to sum up the power from various modules (Figure 3).

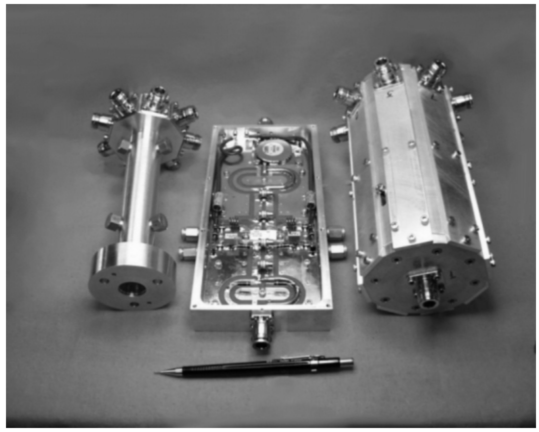

Figure 3: Prototype solid state amplifier module and power combiner/dividers. This module produced 250 W @ 476 MHz.

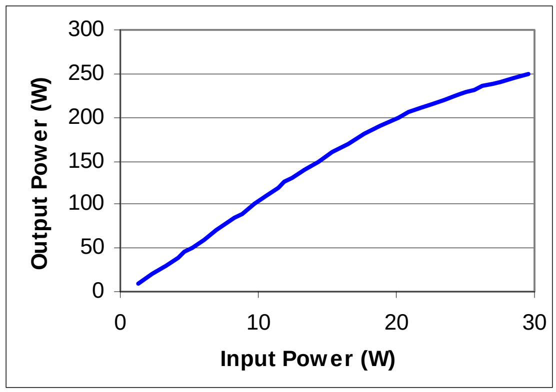

Figure 4: Prototype amplifier module gain curve @ 476 MHz.

7 CONCLUSIONS

The construction of all subsystems for the LNLS 500 MeV booster synchrotron is well advanced and installations should be completed by the end of this year. Commissioning will start in January 2001.

REFERENCES

[1] A.R.D. Rodrigues et al, *Design of a Booster for The Brazilian Synchrotron Light Source*, EPAC 98, Stockholm, Sweden.

[2] T. Ruan, J.M. Godefroy, J. Polian, F. Ribeiro, *500 MHz 1 kW CW Mosfet Amplifier*. Super-Aco/98-03.